Solar Energy Materials 12 (1985) 57–68
North-Holland, Amsterdam

TRANSPARENT CONDUCTIVE $CdIn_2O_4$ THIN FILMS PREPARED BY DC REACTIVE SPUTTERING

K. BUDZYŃSKA and E. LEJA

Department of Solid State Physics, Academy of Mining and Metallurgy, al. Mickiewicza 30, 30-059 Kraków, Poland

S. SKRZYPEK

Department of Physical Metallurgy, Academy of Mining and Metallurgy, al. Mickiewicza 30, 30-059 Kraków, Poland

Received 1 November 1984

Transparent conductive $CdIn_2O_4$ thin films were prepared by dc reactive sputtering from a Cd–In alloy target in an $Ar–O_2$ atmosphere. The highest conductivity found for cadmium indate films was 3700 Ω^{-1} cm^{-1}, (sheet resistance $R_\square = 5\ \Omega$) with a carrier concentration n of 4×10^{20} cm^{-3} and a mobility μ_H of 57 cm^2 V^{-1} s^{-1} under optimized technological conditions. The average optical transmission in the visible region of the light spectrum was 90% for 1 μm thick films. All the films prepared contained the cubic spinel phase of $CdIn_2O_4$ while a secondary phase of In_2O_3 was also present. A carrier scattering mechanism was proposed. The optical band gaps for direct allowed and direct forbidden transitions were derived from the absorption data. The effect of post-deposition heat-treatment in a reducing atmosphere was also investigated.

1. Introduction

Cadmium indate, $CdIn_2O_4$ belongs to a group of broad-band-gap semiconductors that shows the remarkable property of being highly conductive while still transparent in the visible region of the light spectrum. The great attention being paid to transparent conductive coatings seems from their wide range of applications, e.g. in optoelectronics [1,2] and in solar energy conversion technology [3–6]. These films can be used as transparent electroheaters, antistatic layers or transparent electrodes in solar cells. Up to now In_2O_3:Sn and Cd_2SnO_4 films have been extensively studied [7–23]. Th next attractive material, i.e. $CdIn_2O_4$, with an electrical conductivity as high as 4500 Ω^{-1} cm^{-1} and a transmission of about 90% in the visible region of the spectrum, has been prepared recently [24] by rf sputtering from a hot pressed powder target.

In this paper we report on $CdIn_2O_4$ thin films prepared by dc reactive sputtering from a Cd–In alloy target in an $Ar–O_2$ reactive gas mixture. The purpose of our work was to determine structural and electrical properties of deposited films as well as to demonstrate the usefulness of this preparation method. The effect of post-deposition annealing in a reducing atmosphere on the physical properties of the prepared films was also investigated.

As a complete analysis of the optical properties of $CdIn_2O_4$ films, concerning the influence of the preparation conditions and post-deposition heat-treatment on the behaviour of optical coefficients, will be presented elsewhere, only some aspects of the optical investigations are included in this paper.

2. Experimental

Samples were prepared by dc reactive sputtering from a 66 at% In + 34 at% Cd alloy target at different oxygen concentrations in an $Ar-O_2$ atmosphere. The sputtering system is described in detail elsewhere [25]. Thin films were deposited on Corning 7059 cleaned glass substrates mounted to the water cooled sample holder equipped with a heater. Substrates were heated at 473 K for 15 min in vacuum before the sputtering was performed. Oxygen and argon were introduced into the sputtering chamber independently through needle valves. After admitting oxygen and argon to a predetermined pressure, presputtering of the target onto the target shutter was performed. Films were prepared under the following conditions:

target-to-substrate spacing:	35 mm,
discharge current density:	1.05–1.66 mA/cm^2,
discharge voltage:	2000 V,
total pressure:	6 Pa,
pumping rate:	0.002 m^3/c,
presputtering time:	30 min,
deposition time:	1 h.

Samples for electrical and optical measurements as well as for composition, structure and thickness determination were deposited simultaneously. The film thickness was determined using a Talysurf 4 profilometer. The growth rate of the films was analysed as a function of the oxygen concentration in the reactive gas mixture (fig. 1). The growth rate of the films does not show any remarkable

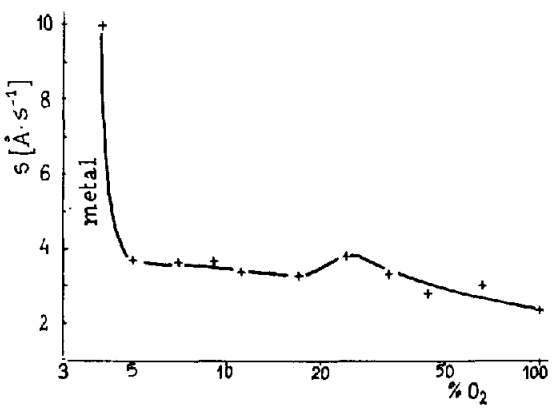

Fig. 1. Film growth rate vs. the oxygen concentration in an $Ar-O_2$ mixture.

dependence on the oxygen content in an $Ar-O_2$ mixture for the range of oxygen concentrations in which oxide compounds are formed. An abrupt increase in the growth rate from 3 to 10 Å/s occurs when the sputtering is assumed to be of metallic character, i.e. when mixed metal-oxide films are formed during deposition. The critical value of the oxygen concentration at which the sputtering changes its character corresponds to that reported for In_2O_3: Sn and Cd_2SnO_4 [20,26].

In order to determine the film composition, X-ray electron microprobe analysis was performed. The measurements were carried out using an ARC SEMQ microanalyser with an accuracy of 2%. The crystal structure of the deposited films was investigated using the X-ray diffraction method with CoK_α radiation filtered through an Fe foil. The surface morphology was investigated by scanning electron microscopy. The optical transmission and reflection were measured as a function of the wavelength from 0.33 to 0.9 μm by a Zeiss UV-VIS double spectrophotometer. The reflection was measured relative to a clean quartz plate. Conventional Hall measurements were performed in the temperature range from liquid nitrogen temperature to 373 K. The chosen samples were subjected to post-deposition heat-treatment in hydrogen at 673 K for 2 h. The process of reduction was carried out at constant hydrogen flow and at constant pressure $p = 0.01$ Pa.

3. Results and discussion

3.1. Composition and crystal structure

Electron X-ray microprobe analysis revealed that all films prepared were nearly of the same composition: 58 wt% In + 26 wt% Cd + 16 wt% O. An indium-to-cadmium atomic ratio of 2.2 was detected in films, while that of oxygen-to-cadmium was lower than 4. It suggest that non-stoichiometric, oxygen-deficient films were obtained. The indium-to-cadmium atomic ratio, apparently higher than that required

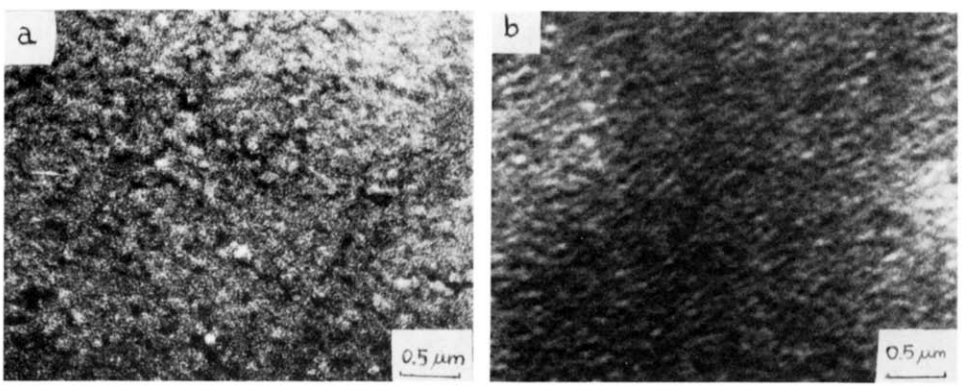

Fig. 2. Scanning electron micrographs for films deposited onto glass substrates: a: at 100% of oxygen; b: at 7% of oxygen.

for stoichiometric cadmium indate, resulted in formation of a secondary separate phase of In_2O_3, as proven by X-ray diffractometer measurements. However, it should be noted that the samples contained a majority of the $CdIn_2O_4$ phase while only small concentrations of In_2O_3 were detected. No X-ray line corresponding to the other possible phases, e.g. of CdO, was observed in all films deposited. However, the possibility that amorphous inclusions of CdO are formed and hence not detected by X-ray diffraction, cannot be ruled out.

Two different crystallographic structures of cadmium indate are reported in

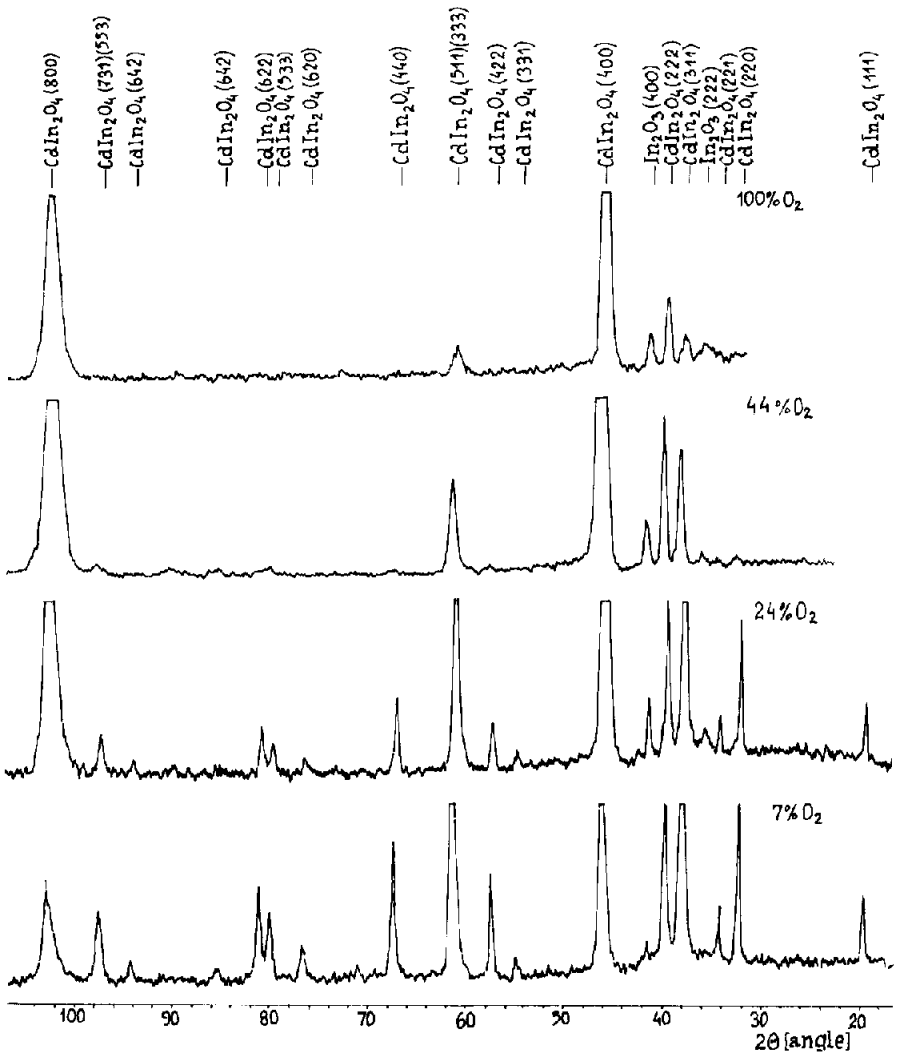

Fig. 3. X-ray diffraction patterns (CoK_α radiation) for samples deposited at various oxygen concentrations in an $Ar-O_2$ mixture.

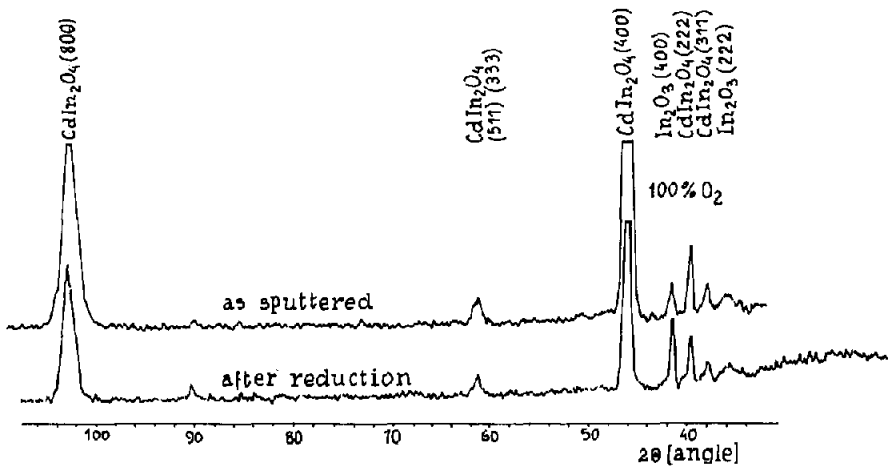

Fig. 4. X-ray diffraction patterns (CoK_α radiation) for samples deposited at 100% of oxygen in a reactive gas mixture, showing the difference between as-sputtered and heat-treated films.

literature: tetragonal with lattice constants $a = 8.65$ Å, $c = 9.87$ Å [27] and cubic spinel with $a = 9.11$ Å [28]. We found that the cubic spinel structure was formed in all films deposited with a slightly greater lattice constant than that mentioned above. All films deposited were polycrystalline with a grain size of about 500–700 Å, as indicated by scanning electron micrographs and an analysis of the half-full width of X-ray diffraction peaks. Scanning electron micrographs for typical films are presented in fig. 2.

X-ray diffraction patterns for films prepared at different oxygen concentrations are demonstrated in fig. 3. Films obtained at high oxygen concentrations show a distinct ⟨100⟩ texture perpendicular to the substrate surface. The occurrence of the preferred ⟨100⟩ orientation may be connected with a high substrate temperature induced by plasma heating [22]. It seems certain that observed changes in the number and intensities of X-ray diffraction lines are not only due to the oxygen variation, as the composition of the $Ar–O_2$ mixture in dc sputtering strongly affects the substrate temperature. Post-deposition heat-treatment does not lead to fundamental changes in the crystal structure of the films but enhances ordering processes followed by an increase in the degree of texture (fig. 4). An increase in the grain size for both the $CdIn_2O_4$ and the In_2O_3 phase in samples subjected to the post-deposition heat-treatment is seen in fig. 4.

More work is still needed in order to determine the influence of both the oxygen concentration during deposition and the post-deposition annealing on the lattice constant, degree and type of texture as well as on the quantitative phase composition.

3.2. Electrical properties

The room-temperature electrical conductivity was studied as a function of the oxygen concentration in the reactive gas mixture. Results for as-sputtered and

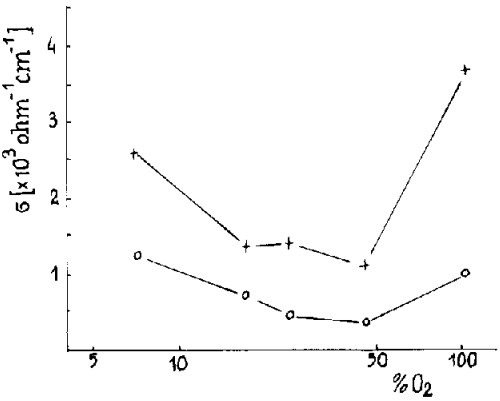

Fig. 5. The electrical conductivity of films sputtered from a 66 at% In + 34 at% Cd target as a function of the oxygen concentration in an $Ar-O_2$ mixture: ○: as-sputtered films, +: after reduction in hydrogen.

heat-treated films are presented in fig. 5. A broad minimum in conductivity is observed for an oxygen concentration within the range of 20 to 60%. In order to explain this behaviour the Hall measurements were performed. The Hall mobility μ_H and the carrier concentration n were determined and plotted versus the oxygen concentration (figs. 6 and 7). The Hall mobility is strongly affected by sputtering conditions and post-deposition heat-treatment while the carrier concentration, although increasing slightly with decreasing oxygen concentration, is almost insensitive to the subsequent annealing in a reducing atmosphere. The maximal difference in carrier concentration between as-sputtered and heat-treated films is observed for samples deposited at oxygen concentrations higher than 40%. However, in this range of oxygen concentrations the substrate temperature abruptly increases (for details see ref. [22]) and the explanation of changes in the electrical parameters (σ, μ_H, n)

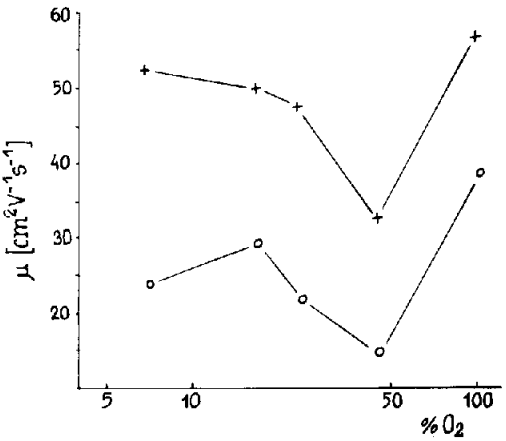

Fig. 6. The Hall mobility of films obtained by sputtering from a 66 at% In + 34 at% Cd target as a function of oxygen concentration: ○: as-sputtered films, +: after reduction in hydrogen.

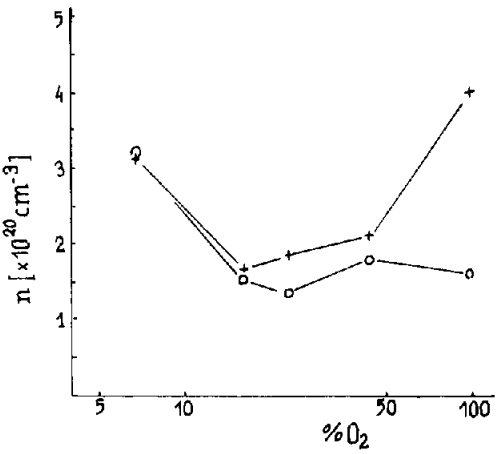

Fig. 7. The carrier concentration of films obtained by sputtering from a 66 at% In + 34 at% Cd target as a function of oxygen concentration: O: as-sputtered films, +: after reduction in hydrogen.

should involve two factors: oxygen concentration and substrate temperature. The carrier concentration of the order of 10^{20} cm^{-3} observed independently of the sputtering conditions may be accounted for by the high density of ionized point defects generated during deposition. Hall measurements performed in a wide temperature range revealed that the films deposited are highly degenerate n-type semiconductors (see fig. 8). Therefore, it can be proposed that donation of free electrons is caused by vacancies in the anion sublattice (oxygen vacancies) and interstitial atoms resulting from disorder in the cation sublattice. The existence of these types of defects in undoped oxide semiconductors is generally accepted in literature [15,18,29,30]. As sputtering plasma with a low oxygen content favours generation of oxygen vacancies, the carrier concentration increase with decreasing oxygen concentration below 30% of oxygen can be attributed to an increase in the

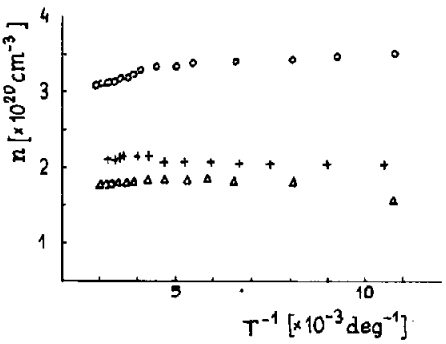

Fig. 8. Temperature dependence of the carrier concentration for films: △: as-sputtered deposited at 45% of oxygen, +: reduced in hydrogen after deposition at 45% of oxygen, O: as-sputtered deposited at 7% of oxygen.

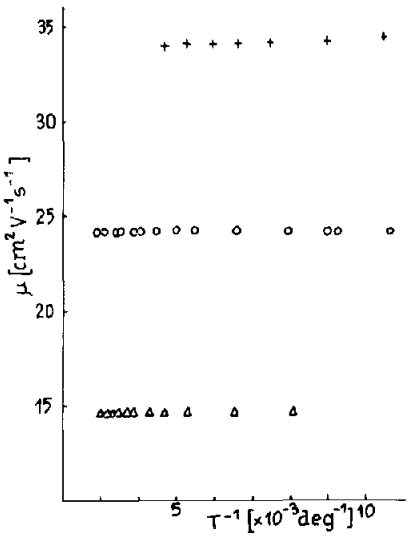

Fig. 9. Temperature dependence of the Hall mobility for films: △: as-sputtered deposited at 45% of oxygen, +: reduced in hydrogen after deposition at 45% of oxygen, ○: as-sputtered deposited at 7% of oxygen.

density of oxygen vacancies. The fact that above 30% of oxygen the carrier concentration does not decrease any longer may be explained in terms of the substrate temperature increase. In view of the high level of degeneracy it is not surprising that the carrier concentration cannot be considerably enlarged by a subsequent annealing in a reducing atmosphere. As reduction in hydrogen mainly affects the density of oxygen vacancies, the increase in carrier concentration can be seen only for samples partially oxidized. Thus the additional generation of oxygen vacancies due to the post-deposition heat-treatment can occur for films obtained previously in an oxygen-rich atmosphere.

As far as the Hall mobility dependence on the oxygen concentration in a reactive mixture is concerned, it should be noted that two processes are usually taken into account: charge carrier scattering, which reduces the Hall mobility, and structure ordering, acting inversely. Thus the high Hall mobility at 100% of oxygen can be attributed to a low degree of disorder resulting from a high substrate temperature and confirmed by X-ray diffraction studies. A small decrease in the Hall mobility with increasing carrier concentration below 20% of oxygen seems to be a result of charge carrier scattering. However, the reasons for the occurrence of the Hall mobility minimum seen in fig. 6 are not fully understood yet. The formation of some neutral defects can be postulated in this range of concentrations but additional experimental evidence is necessary before this assumption will be confirmed.

A significant increase in the electrical conductivity, from 1000 Ω^{-1} cm^{-1} for as-sputtered films to almost 4000 Ω^{-1} cm^{-1} for films subjected to hydrogen reduction, seems to be mainly a consequence of an increase in Hall mobility (from

30 to 50 $cm^2\ V^{-1}\ s^{-1}$). As far as the electrical conductivity of dc sputtered films is being considered, we believe that the ordering processes occurring during annealing play a much more important role than the additional generation of charge carriers.

In order to determine the character of the scattering mechanism of the charge carriers, the temperature dependence of the Hall mobility was plotted for some chosen samples (fig. 9). The specific character of the plot suggests that the charge carrier scattering at ionized point defects is the predominant scattering mechanism in all films deposited.

3.3. Optical properties

The optical transmittance T and the reflectance R were determined in a wide range of the light spectrum in order to derive optical constants, i.e. the extinction coefficient k (or absorption coefficient α) and the refractive index N, versus the frequency of incident radiation. In fig. 10 the optical transmission and reflection for an as-sputtered and then heat-treated film are presented. All films prepared showed a high transmittance ($T \simeq 90\%$) combined with a comparatively low reflectance ($R \simeq 10\%$) in the visible region of the spectrum.

Calculations of the optical constants were performed using a method proposed in ref. [31]. The frequency dependence (for simplicity energy units were used) of the

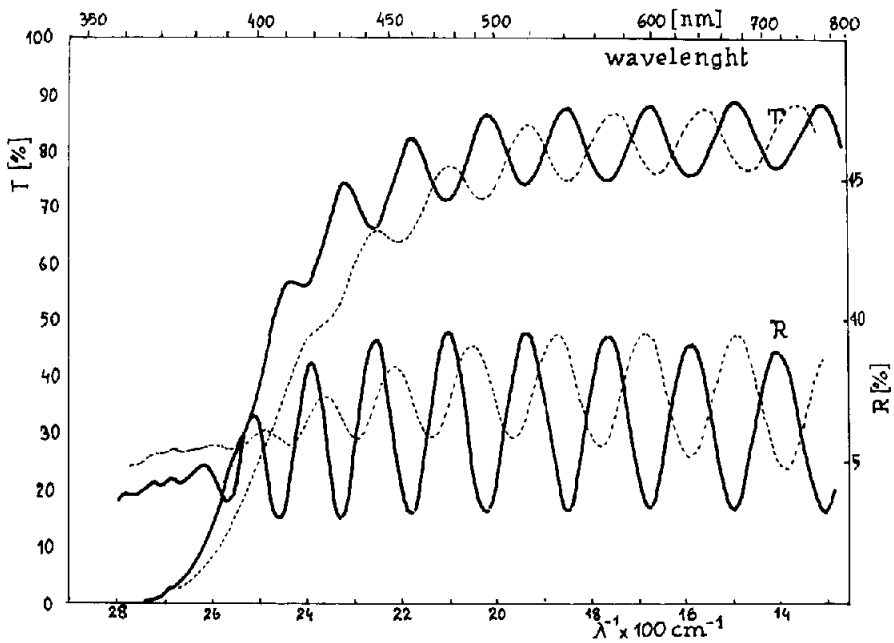

Fig. 10. Optical transmission (left scale) and reflection (right scale) spectra for a film obtained at 45% of oxygen in an $Ar-O_2$ mixture: dashed line: as-sputtered film with $R_\square = 20\ \Omega$; solid line: reduced in hydrogen ($R_\square = 8\ \Omega$). The film thickness was 1.15 μm.

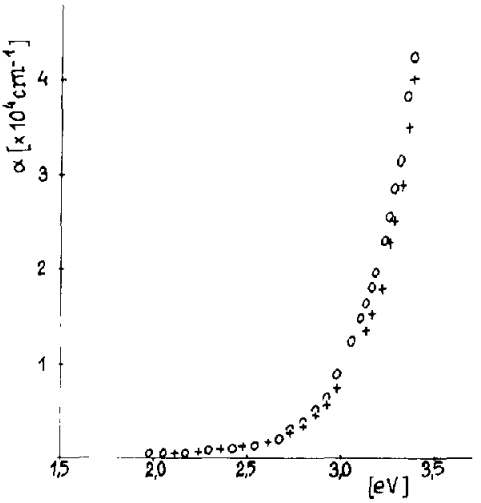

Fig. 11. The absorption coefficient, α, vs. the photon energy for the film deposited at 45% of oxygen in an $Ar-O_2$ mixture: O: as-sputtered, +: after reduction in hydrogen.

absorption coefficient α for a typical sample is shown in fig. 11. The average refractive index for this sample was found to be 2.10. Plotting $(\alpha E)^2$ and $(\alpha E)^{2/3}$ as a function of the photon energy we were able to fit two straight lines, respectively, to the experimental data. The intercepts of these lines with the photon energy axis give optical energy gaps: $E_g = 3.24$ eV for direct allowed transition and $E_g = 2.23$ eV for direct forbidden transition. These values of the energy gaps and the observed optical transitions remain in good agreement with those obtained from photoelectrolysis spectra of $CdIn_2O_4$ [32]. A small shift in the position of the absorption edge towards higher frequencies, probably resulting from the increase in the carrier concentration, was also observed in the absorption spectra of reduced films.

4. Conclusions

Electrical and structural properties of $CdIn_2O_4$ thin films deposited by dc reactive sputtering from a 34 at% Cd + 66 at% In alloy target were found to be dependent upon the oxygen concentration in the reactive gas mixture during deposition as well as on the post-deposition heat-treatment in a reducing atmosphere.

X-ray diffractometer measurements revealed that the cubic spinel phase of $CdIn_2O_4$ prevailed in the prepared films while the secondary phase of In_2O_3 was also present.

Cadmium indate thin films prepared by dc reactive sputtering are highly degenerate n-type semiconductors with a carrier concentration as high as 4×10^{20} cm^{-3}. A high density of point defects, i.e. oxygen vacancies and interstitial Me atoms, along with a high Hall mobility of charge carriers, is responsible for the high electrical

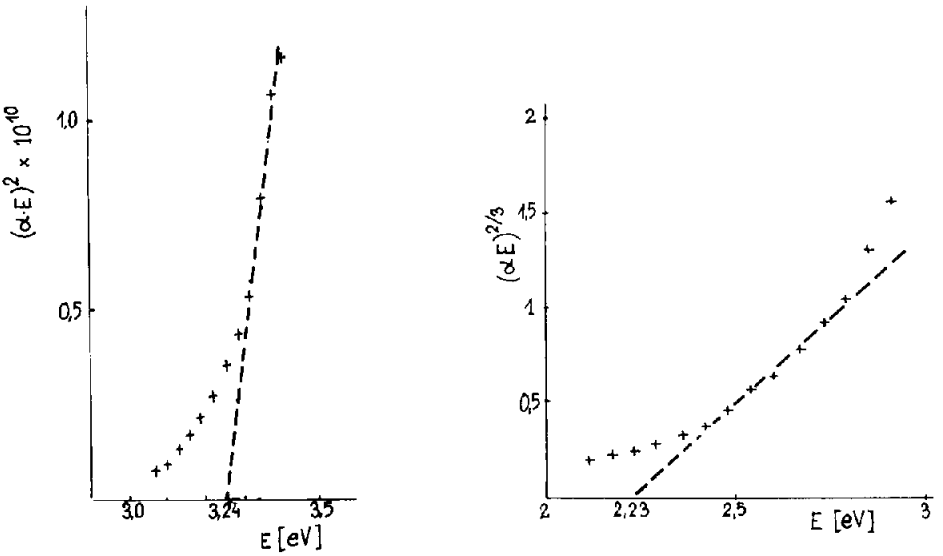

Fig. 12. $(\alpha E)^2$ as a function of the photon energy E for the film obtained at 45% of oxygen, indicating direct allowed optical transition with energy $E_g = 3.24$ eV.

Fig. 13. $(\alpha E)^{2/3}$ as a function of the photon energy E for the film obtained at 45% of oxygen, indicating a direct forbidden optical transition with energy $E_g = 2.23$ eV.

conductivity of those films. Hall mobility behaviour indicates that ionized point defects play a dominant role in the carrier scattering mechanism.

Films with high optical transmission ($\simeq 90\%$) in the visible region of the light spectrum were prepared. From an analysis of optical coefficients (figs. 12 and 13), two types of optical transitions were deduced.

Taking into account the film properties presented in this paper we conclude that thin films of $CdIn_2O_4$ prepared by dc reactive sputtering from an Cd–In alloy target seem to be promising candidates for application as transparent electrodes in solar energy elements.

Acknowledgements

We would like to acknowledge the assistance of T. Horodyski in performing the electrical measurements. Our thanks are due to H. Czternastek for carrying out optical investigations. We are indebted to Dr. L. Maksymowicz for valuable discussions.

References

[1] Y.T. Sihvonen, and D.R. Boyd, Rev. Sci. Instr. 31 (1960) 992.
[2] R.R. Mehta and S.F. Vogel, J. Electroch. Soc. 119 (1972) 752.
[3] J.C.C.Fan and F.J. Bachner, Appl. Opt. 15 (1976) 1012.
[4] J.C. Manifacier, L. Szepessy, J.F. Bresse, M. Perotin and R. Stuck, Mat. Res. Bull. 14 (1979) 163.
[5] G. Frank, E. Kauer, H. Kostlin and F.J. Schmitte, Proc. SPIE 324 (1982) 58.
[6] C.M. Lampert, Proc. SPIE 324 (1982) 1.
[7] H.K. Muller, Phys. Stat. Sol. 27 (1968) 723.
[8] A.J. Nozik, Phys. Rev. B6 (1972) 453.
[9] G. Haacke, Ann. Rev. Mater. Sci. 7 (1977) 73.
[10] L.A. Siegel, J. Appl. Cryst. 11 (1978) 284.
[11] G. Haacke, W.E. Mealmaker and L.A. Siegel, Thin Solid Films 55 (1978) 67.
[12] C.E. Wickersham and J.E. Greene, Phys. Stat. Sol. (a) 47 (1978) 329.
[13] J.E. Morris, M.I. Ridge, C.A. Bishop and R.P. Howson, J. Appl. Phys. 51 (1980) 1847.
[14] N. Miyata, K. Miyake and Y. Yamaguchi, Appl. Phys. Lett. 37 (1980) 180.
[15] M. Mizuhashi, Thin Solid Films 70 (1980) 91.
[16] J.N. Avaritsiotis and R.P. Howson, Thin Solid Films 77 (1981) 351.
[17] R.P. Howson, M.I. Ridge and A. Bishop, Thin Solid Films 80 (1981) 137.
[18] G. Frank and H. Kostlin, Appl. Phys. A27 (1982) 197.
[19] L. Gouskov, J.M. Saurel, C. Gril, M. Boustani and A. Oemry, Thin Solid Films 99 (1983) 365.
[20] E. Leja, K. Budzyńska, T. Pisarkiewicz and T. Stapiński, Thin Solid Films 100 (1983) 203.
[21] H.S. Soni, S.d. Sathaye and A.P.B. Sinha, Indian J. Pure Appl. Phys. 21 (1983) 197.
[22] T. Horodyski, K. Budzyńska and E. Leja, Thin Solid Films 106 (1983) 195.
[23] T. Stapiński and E. Leja and T. Pisarkiewicz, J. Phys. D17 (1984) 407.
[24] G. Haacke, Proc. SPIE 324 (1982) 10.
[25] E. Leja, J. Korecki, K. Krop and K. Toll, Thin Solid Films 59 (1979) 147.
[26] E. Leja, A. Kołodziej, T. Pisarkiewicz and T. Stapiński, Thin Solid Films 76 (1980) 283.
[27] L. Passerini, Gazz. Chim. Ital. 60 (1930) 754.
[28] M. Skribljak, S. Dasgupta and A.B. Biswas, Acta Cryst. 12 (1959) 1049.
[29] J.A. Marley and R.C. Dockerty, Phys. Rev. 140 (1965) 304.
[30] R.D. Shannon, J.L. Gillson and R.J. Bouchard, J. Phys. Chem. Solids 38 (1977) 877.
[31] J. Szczyrbowski and A. Czapla, J. Phys. D12 (1979) 1737.
[32] F.P. Koffyberg and F.A. Benko, Appl. Phys. Lett. 37 (1980) 320.